EFFECT OF TWINNING ON TEXTURE EVOLUTION OF DEPLETED URANIUM USING A VISCOPLASTIC SELF-CONSISTENT MODEL

A Thesis
Presented to
The Academic Faculty

By

John Ho

In Partial Fulfillment
Of the Requirements for the Degree
Master of Science in the
School of Materials Science and Engineering

Georgia Institute of Technology

August, 2012

EFFECT OF TWINNING ON TEXTURE EVOLUTION OF DEPLETED URANIUM USING A VISCOPLASTIC SELF-CONSISTENT MODEL

Dr. Hamid Garmestani
School of Materials Science and Engineering
Georgia Institute of Technology

Dr. David McDowell
School of Materials Science and Engineering
Georgia Institute of Technology

Dr. Richard Neu
School of Materials Science and Engineering
Georgia Institute of Technology

Date Approved:

ACKNOWLEDGEMENTS

TABLE OF CONTENTS

Page

LIST OF TABLES

LIST OF FIGURES

NOMENCLATURE

$\mathbf{B}^c$: Accommodation Tensor

b: Unit Vector in slip direction

CRSS: Critical Resolved Shear Stress

D: Applied Polycrystal Strain Rate

DU: Depleted Uranium

$\dot{\mathbf{E}}$: Imposed Macroscopic Strain Rate

$\dot{\mathbf{E}}^0$: Reference Strain Rate of HEM

FCC: Face-Centered Cubic

F_E : "Effective" polycrystal twinned fraction

F_R : "Real" polycrystal twinned fraction

F_T: Twin reorientation threshold

f^n : Volume fraction representing a grain that is completely reoriented by twinning

$g^{n,ti}$: Fraction of the grain associated with a twin system, t_i

HEM: Homogeneous Equivalent Medium

HF: Hydrogen Flouride

K_1: Twinning Plane

LApp: Los Alamos Polycrystal Plasticity Model

$M^{(sec)}$: Overall viscoplastic compliance moduli of the grain

$\mathbf{M}^{(sec)}$: Macroscopic Secant Modulus

$\mathbf{M}^{(tg)}$: Viscoplastic Compliance of HEM

$\mathbf{M}^{c(tg)}$: Viscoplastic Compliance of polycrystal

$\tilde{\mathbf{M}}$: Interaction Tensor

n: Rate Sensitivity Exponent

n: Slip System Unit Normal Vector

RC: Relaxed Constraints Model

S: Characteristic shear of a twin

S: Eshelby Tensor

S: Plane of Shear

S: Antisymmetric component of the plastic distortion rate (plastic spin)

t_i: Twin system

U-235: Uranium-235

U-238: Uranium-238

UTS: Ultimate Tensile Strength

VFT: Volume Fraction Transfer Scheme

VPSC: Viscoplastic Self-Consistent Model

$\dot{\gamma}_o$: A reference shearing rate

$\dot{\gamma}^s$: Inelastic strain rate associated with the shearing rate on the sth slip system

$\Delta g^{n,ti}$: Volume fraction of grain n

$\Delta \gamma^{n,ti}$: Shear strain contributed by the twinning system t_i in grain *n*

Δt : Time Interval

$\dot{\boldsymbol{\varepsilon}}$: Strain Rate

$\dot{\boldsymbol{\varepsilon}}^0$: Reference Strain Rate of polycrystal

$\dot{\boldsymbol{\varepsilon}}^*$: Transformation Strain Rate

η_1: Twinning Direction

Π : Reorientation of an associated ellipsoid (grain)

$\boldsymbol{\sigma}$: Stress within each grain

τ^s_{crit} : Critical Resolved Shear Stress for the sth slip system

τ^s_r : Resolved shear stress of the sth system

$\dot{\Omega}$: Antisymmetric component of the macroscopic distortion rate

SUMMARY

Depleted uranium, a low symmetry material with a high propensity for twinning, was investigated in study to simulate the texture evolution during mechanical deformation. Simulations of several different processing methods, such as compression, swaging, rolling and torsion, were applied using a viscoplastic self-consistent model. These simulations were used to analyze texture evolutions of the uranium, starting from a randomly oriented sample. The textures from these simulations were plotted as both pole figures and inverse pole figures, which were compared and validated against experimental data from previous works on uranium. As these simulations were made to eventually create process paths for improving mechanical properties of uranium, specific exploration was made for the (176)[512] twin. This twin has been found to be a major strengthening mechanism for the fracture toughness of uranium. As such, deformational simulations were made with this twin active and not active, and comparisons between the two were made. In general, it was found that the (176)[512] twin impeded the growth of texture intensity in most samples. Finally, a processed uranium sample from Y12 was analyzed. This sample's specific processing history was unknown, but a simulated deformation process which consisted of 100% compression with only the {110}<110> slip and (176)[512] twin systems having been active was able to satisfactorily match the experimental texture.

INTRODUCTION

Although once popular as a material of research following the Second World War, information on the material properties of uranium are now hard to come by. Much of the information is old and outdated, or even impossible to find. This paper hopes to be a part of a new resurgence in the research of uranium properties. Depleted uranium is once more becoming a material of interest as a structural material, but many properties of the material are not well known, such as fracture toughness. In order to begin to understand how to use uranium as a structural material, vital research must be done to know how the material will react to stresses, which ways to process the uranium to produce the properties that are favorable, and which applications the material can be useful for. As a method of practically designing the applications of uranium, a process path would be very useful in this endeavor. The method chosen to approach this endeavor is to model the different deformational processes that could be underdone to the uranium and then map its textural evolution. The texture of a material often has a vital correlation to its mechanical properties. It is hoped that the use of the modeling and simulations done in this paper will allow for further exploration into how specific textures can be achieved via certain processing methods, which would then lead to improvements in material properties selection and post-processing.

CHAPTER 2

2.1 Background

Uranium is the heaviest naturally occurring element in nature [1]. It's natural decay cycle has it stripping itself of two protons and two neutrons becoming radium, radon, polonium, and continuing onward until finally becoming stable once the element ends at lead [1]. The half life of radioactive uranium-235 is 4.5 billion years [1]. Naturally occurring uranium is very stable and in too low a concentration to trigger a nuclear reaction. The concentration of U-235 has to be above 20 percent for it to have the possibility of a spontaneous reaction [1]. The much more common isotope which makes up the bulk of naturally occurring uranium is U-258. When the natural uranium ore is "enriched," the U-235 isotope is separated from the U-258 and concentrated together. The U-238 isotope which is left over, and which has a much lower radioactivity and reactivity, is commonly known as "depleted" uranium — or uranium ore which has been depleted of U-235. Before being used as a radioactive source for weaponry or power production, naturally occurring uranium was used for much more domestic applications. Uranium has been used as a colorant for pigments, a tinting agent for glasses, and the source of the deep red dyed color of Fiesta Ware dishes [1]. Until the use of uranium as the keystone of nuclear weaponry, it had very little value.

Uranium pricing reached a peak in the 1970s as nuclear power and atomic weaponry held great interest for civilian and military application, but steadily declined afterwards due to

slow growth in the nuclear power industry. The price of uranium continued to decline through 2000, although there was a brief rebound in 2005 [2]. The modern exploration of uranium began in the 1940s for military applications, but shifted to a civilian focus in the 1950s as nuclear power gain importance [2]. The uranium economy of the United States remained optimistic, and uranium production continued to grow as it was perceived that nuclear power was the "power of the future." However, the Three Mile Island accident of 1979 halted the interest in uranium as a power source for many years [2]. As military demand dropped after the Cold War, further interest in uranium production dropped even lower [2].

Uranium was thought of as waste product in the search for radium, which at the time was very valuable for medicinal uses [1]. The raw uranium ore was only mined because the more precious radium metal was usually found lodged within the uranium. Miners during the 1500s called it "pitchblende," and regarded it as a sign of a silver mine having been dried up, leaving nothing but a "garbage" mineral [1]. Although the first mining "boom' of uranium started with the discovery of radium within uranium veins, uranium itself was the focus of mining once Otto Hahn discovered the fissionable properties of uranium in 1938 [2]. The process of fission opened the doors of uranium being of possible use in military, as well as civilian power, applications [2]. The modern name "uranium" was given to the element by a Berlin pharmacist named Martin Klaproth, who was able to isolate the uranium from the waste pitchblende, after the recently discovered planet Uranus [1].

In order to refine this mixture, one of two methods is typically used: leeching by either sulfuric acid or sodium carbonate. The acid leeching method is more efficient and does not require fine milling of the ore, but the sodium carbonate process is more specific for uranium. It also prevents large acid losses if the raw ore contains acid-neutralizing components. After the leeching process, the pitchblende mixture is converted into another oxide, UO_3. This oxide is further processed with HF to produce UF_4, which is the form usually used for long term storage of uranium. The UF_4 is finally reduced with magnesium to produce pure uranium. The uranium, however, is a mixture of different isotopes—mainly U-235 and U-238. As the two isotopes have different molecular weights, the uranium is turned into a gaseous state and then separated by diffusion or centrifuge [3].

Depleted uranium is a by-product of the enrichment process of raw uranium ore. The raw ore is mostly composed of U_3O_8, with 1% to 60% uranium, although US deposits are typically only 0.6% to 6% uranium [3]. Once the two isotopes are separated, the enriched U-235 isotope can be used as a fissionable material. The remainder possesses a mixture of less than .711% U-235 and the rest being U-238. This by-product is depleted uranium (DU or DU-238), called so because the material has been depleted of most of the fissionable product. While DU itself is not fissionable, it can be reacted to produce fissionable plutonium [4]. Because of the very low concentration of U-235, however, DU is not able to directly produce nuclear chain reactions. Most applications of DU do not

use its radioactive properties and instead make use of its high density. DU is mildly radioactive, emitting alpha radiation, but the more powerful gamma radiation cannot leave the material itself. Because of the very low concentration of the gamma emitting U-235, the radiation gets absorbed before it can leave the material [5].

Although depleted uranium is primarily used for its radioactive properties, it has many applications as a structural material, such as shielding and projectile penetration which exploits its high density of 19.1 g/cm^3. The strength of DU is moderate, with a UTS of 650 MPa and a yield strength of 220 MPa, which is less than steel [6]. Cast, unalloyed DU is moderately brittle, with a high elastic modulus, 172 GPa, and a low elongation (1% to 5%). These mechanical properties limit structural applications, although DU is used for casks and containers that exploit its radioactive shielding properties [7]. DU has the same crystal structure as α-uranium, with a high propensity for twinning during mechanical deformation. Twinning may be treated as a "shuffling" mechanism, where lattice cells can "shuffle" into a twinned plane, rather than undergoing homogeneous shear, slip and rotation. For complex lattice structures, high shear stress can produce twinning via very simple shuffling mechanisms, while lower shear stress can promote complex shuffling. With a double lattice structure, α-uranium can exhibit twinning at low shear stresses based on these shuffle mechanisms [8].

2.2 Texture

Texture is the prevalence of a preferred orientation for the component crystals in a multi-crystal, or polycrystal, material. This property of a polycrystal, measured as one for a completely randomly oriented material – i.e., a non-textured material – and increasing as the crystal grains become more singularly oriented in a specific direction, is an important parameter to determine the anisotropy of a material. Nearly every mechanical property of interest in a polycrystal, such as chemical resistance or fracture toughness, is anisotropic, so the textural properties of these materials are of great importance [9]. While the Taylor model of polycrystal deformation is adequate for use with single phase cubic lattices [9], it is not quite adequate for use with low symmetry materials, such as alpha-phase uranium. In order to correctly predict material behaviors and properties, the single crystal properties of a material must by correctly averaged to account for the anisotropy of the polycrystalline form, and the mechanical grain interactions must also be considered.

Texture is also useful as evidence to the types of processing a material has been through. Much of the actual ways that texture is generated, as in the distribution of the oriented grains, is a result of the methods by which the material was manufactured [9]. This linkage between the texture that a type of processing induces in a material and the anisotropic material properties that a certain texture influences is instrumental in creating an efficient process path design of a material. Optically and chemically, a material may seem identical, but differences in texture can lead to dramatic changes in mechanical

properties [9]. Materials of low ductility have a high correlation between texture and fracture toughness [9]. Because uranium is such a material, the texture of the material is an important aspect to note when one is trying to improve its fracture toughness.

2.3 Twinning

There are two types of deformation which contribute to plastic, or permanent, deformation: slip and twinning. In slip, the top half of a plane glides over the bottom half, moving atoms in whole numbers of lattice vectors. Contrarily, during twinning, whole lattice vector movements are not obtained, but instead the twinned region will by over several planes with each atom being moved an amount relative to those beneath them [10]. During both the slip and twin processes, the lattice structure is preserved; however, while twinning keeps the lattice structure, it turns it into a different orientation [11]. This allows for a material which undergoes twinning to preserve both its crystal symmetry and crystal structure [12]. As the stress to cause twinning is usually high, slip modes of deformation will generally be more prevalent. If there are at least five independent slip systems, deformation by slip will occur and maintain the continuity at grain boundaries. Otherwise, if there is not enough independent slip systems, the material may prematurely fracture. Twinning can, in some materials, alleviate the need for fracture by allowing an additional deformation mechanism for shape change rather than fracture [13].

Twinning is a deformation mode which is more prevalent in low symmetry materials then higher symmetry ones. They can be caused during crystal growth and recrystallization, phase transformations, or by plastic deformation [9]. Twins can be categorized into three types: type I twins occur when a reflection of cells occurs at a habit plane, K_1 – a plane which is the boundary between two particular crystal planes; type II twins occur when there is a 180° rotation about the direction (the twinning direction, η_1) which is the intersection of K_1 and the original plane S – called the plane of shear; and a compound twin occurs when both conditions are satisfied [9].

During deformation twinning, a homogeneous shear parallel to the twinning plane K_1 in the twinning direction η_1, is always the same for a given twin and is called the characteristic twinning shear [9]. A homogeneous shear is one in which the amount of shear increases in proportion to the distance of displacement of the cells caused by the twinning. As the shearing amount to produce a twin is often greater than the amount of shear required to produce slip, slip deformation modes are usually the more common type of deformation. To qualify as a twinning shear, a simple shear must result in a deformation which has the same structure as the parent, but rotated, and in which a single lattice cell of the parent becomes an equivalent cell of the twin [8]. However, certain materials, usually ones of lower symmetry, are able to more easily twin via shuffling mechanisms. Shuffling mechanism allow for materials, which cannot twin via small amounts of shear, to form twin structures without having to simply homogeneously shear every parent atom to the correct twin site [8]. These shuffling mechanisms can be either

composed of a simple shuffling mechanism with a large twinning shear or a complex shuffling mechanism with a small twinning shear [8].

For twinning to occur, the stress to cause the twinning must depend on both the line tension of the source dislocation but also on the surface tension of the twin boundary [10]. As the stress to cause twinning is usually high, slip modes of deformation will generally be more prevalent. However, lower temperatures can increase the amount of twinning, as will materials which have a limited number of slip systems [10]. Oftentimes, twins will only nucleate after slip has already occurred. The pile-up of dislocation caused by slip allow for very high stress concentration where twin nucleation can begin. When twins first nucleate, they appear as thin lamina. Once propagation takes place, a steady migration of the K_1 plane steadily thickens as the twin grows larger [12]. After twins have begun to nucleate, their propagation is much easier and requires much less stress [10].

2.4 Viscoplastic Self-Consistent Model

The complexity of deformation twinning introduces difficulties in the modeling of texture evolution in DU during deformation. A fully described twinning mechanism requires accounting of both twin nucleation and propagation, and associated stress relaxation, twin morphology and its correlation with the parent lattice, and the reoriented twinning fractions [14]. Instead of considering all these factors in detail, Tome and Lebensohn [15] developed a Viscoplastic Self-Consistent (VPSC) model, originally developed by

9

Molinari et al. [16] for an anisotropic polycrystalline material. This model addresses twinning using an approximate volume fraction transfer scheme, where the set of orientations (bins for orientation) are fixed but the associated material volume fractions evolve during the deformation. In other words, the orientation distribution of polycrystalline material is indexed in orientation space, comprised of a set of discrete orientation elements, while the volume fractions of each discrete element evolve during the deformation. Certain volume fractions of the material are assigned to cells (or bins) that represent lattice orientations that define the initial texture. Plastic deformation reorients these cells that represent underlying lattice orientation and displaces them in orientation space. This displacement leads to volume transfer between neighboring unit cells in orientation space. If twinning is activated, then the reoriented fraction is transferred to a corresponding non-neighboring cell [14]. This process is updated at each strain increment to simulate the process of texture evolution.

To study the texture evolution of alpha titanium, Rollett et al. used the LApp (Los Alamos polycrystal plasticity) model [17, 18]. LApp uses an iterative equation solver that can find the stress state and slip distribution for the grains of a polycrystal using a rate-sensitive yield surface [19] and associated flow potential. Assuming fully plastic incompressible flow, the polycrystal strain rate is given by

$$D_{kl} = \sum_s \dot{\gamma}_o m_{kl}^{(s)} \left(\frac{\sigma_{ij} m_{ij}^{(s)}}{\tau_{crit}^s} \right) \left| \frac{\sigma_{qr} m_{qr}^{(s)}}{\tau_{crit}^s} \right|^{n-1}$$

(1)

Assuming the deformation rate to be identical to that of the bulk material in the full constraints mode, five independent nonlinear equations result. In this flow rule, **D** is the applied polycrystal strain rate, $\boldsymbol{\sigma}$ is the stress within each grain, **m**$^{(s)}$ is defined by $m_{ij}^s = b_i^s n_j^s$ for the sth slip system, τ_{crit}^s is the critical resolved shear stress for the sth slip system, n is the rate sensitivity exponent ($\sim$30), and $\dot{\gamma}_o$ is a reference shearing rate [20]. A Relaxed Constraints (RC) model, which deviates from the Taylor model when the grain shape has a large aspect ratio, can account for certain features of FCC rolling textures [21-23]. The RC model in LApp applies a stress boundary condition to the two shear components in uniaxial or plane-strain compression on the rolling plane. When extended to incorporate twinning, Eq. (1) treats twinning as pseudo-slip.

Experimental results were used to validate the simulations. Based on previous work, investigation were made to find the influence of twinning, particularly considering the (176)[512] twin system, on texture evolution of depleted uranium during large deformation. The (176)[512] twin system is not as common as other twin systems in α-uranium under quasi-static deformation, but becomes increasingly dominant when the sample is shocked [24]. The effects of (176)[512] twinning are simulated using the VPSC model, outlined later, and compared with experimental results of a shocked DU sample.

In the VPSC model employed here, it is assumed that the elastic strain is negligible compared to nonelastic strain associated with slip and twinning. It is important to note, however, that in reality active twins produce stress relaxation, inducing potentially substantial redistribution of stress in each grain and surrounding matrix (ensemble of grains with equivalent polycrystalline properties). Elasticity is required to account for this relaxation [15]. The velocity gradient is decomposed into symmetric and skew-symmetric parts, the former associated with inelastic strain rate and the latter with nonelastic spin that drives texture evolution (lattice rotation). The grain orientation distribution is represented by an assignment to a set of weighted orientations. Effects of neighboring grain interactions are therefore not explicitly considered, but rather are implicitly considered in the hardening laws and the character of the self-consistent scheme.

As previously mentioned, the volume fraction transfer scheme (VFT) proposed by Lebensohn and Tome [5] represents the polycrystal using a set of discrete orientations. These orientations are held fixed, while the associated binned volume fractions evolve during deformation. Regularly partitioned (10° Euler angle increment bin size) equiaxed bins of Euler space are assigned in orientation space. Corresponding volume fractions of material are then assigned to cells to represent the initial texture, and slip is then allowed to "displace" the volume fractions of grain orientations in Euler space. This "displacement" essentially represents lattice reorientation. The orientation of each displaces uniformly at each increment, such that it partially overlaps neighboring cells or

bins. This incremental overlap is then subtracted from the original bin and added to the overlapped bins to evolve the texture. In essence, this is a low order approximation that neglects specific intergranular interactions in favor of evolving overall texture to achieve efficiency.

The VPSC model is detailed by Lebensohn and Tome [25], and is summarized here. As mentioned previously, fully plastic deformation is assumed, and it is further asserted that the deformation takes place through shear and is independent of the hydrostatic stress. This allows a five dimensional vector space to be used to in the formulation of inelastic deformation in terms of conjugate deviatoric stress and strain rate tensors. Interchanging two components [25], of the stress and strain convention adopted by Lequeu et al. [26], the stress and strain rate vectors in this five dimensional space are given by

$$\{\sigma'\} = \sqrt{2}\left\{\frac{(\sigma_{33}-\sigma_{11})+(\sigma_{33}-\sigma_{22})}{2\sqrt{3}}, \frac{\sigma_{22}-\sigma_{11}}{2}, \sigma_{23}, \sigma_{13}, \sigma_{12}\right\}^{\mathrm{T}} \tag{2}$$

$$\{\dot{\varepsilon}\} = \sqrt{2}\left\{\frac{(\dot{\varepsilon}_{33}-\dot{\varepsilon}_{11})+(\dot{\varepsilon}_{33}-\dot{\varepsilon}_{22})}{2\sqrt{3}}, \frac{\dot{\varepsilon}_{22}-\dot{\varepsilon}_{11}}{2}, \dot{\varepsilon}_{23}, \dot{\varepsilon}_{13}, \dot{\varepsilon}_{12}\right\}^{\mathrm{T}} \tag{3}$$

The scalar product of these two vectors gives the stress power, i. e.,

$$\sigma'_{k}\dot{\varepsilon}_{k} = \sigma'_{ij}\dot{\varepsilon}_{ij} \tag{4}$$

where it is understood that the sum on subscript k is over the range 1,2,...,5. Inelastic deformation occurs only when a slip and/or twin system is active. Both slip and twin slip systems are characterized by two vectors: the slip systems unit normal vector **n** and the unit vector **b** in the slip direction. Again, twinning is treated in this formulation as pseudo-slip, with the same formulation of the kinematics as crystalline slip.

The resolved shear stress of the sth system, denoted by τ_r^s, is given by

$$\tau_r^s = m_k^s \sigma'_k = m_{ij}^s \sigma_{ij} = m_{ij}^s \sigma'_{ij} \tag{5}$$

where $m_{ij}^s = \dfrac{1}{2}\left(n_i^s b_j^s + n_j^s b_i^s\right)$ is the Schmid tensor.

The inelastic strain rate associated with the shearing rate on the sth slip system, $\dot{\gamma}^s$, is given by

$$\dot{\varepsilon}_k = m_k^s \dot{\gamma}^s \tag{6}$$

The flow rule in Eq. (1) is employed, with the nonlinear viscous relation between the slip system resolved shear stress and shearing rate given by

$$\dot{\gamma}^s = \dot{\gamma}_o \left(\frac{\tau_r^s}{\tau_{crit}^s}\right)^n \text{sgn}\left(\tau_r^s\right) \tag{7}$$

Each grain of the polynomial has the kinematic relation

$$\dot{\varepsilon}_k = \sum_{s=1}^{N} m_k^s \dot{\gamma}^s \qquad (k=1, \ldots, 5) \tag{8}$$

where the summation is carried over all N slip/twin systems in the grain.

The VPSC model couples the strain-rate and the stress in each grain with the average strain rate and stress of the polycrystal [25]. Each grain is regarded as an inhomogeneity embedded in the homogeneous equivalent medium (HEM) having a viscoplastic compliance $\mathbf{M}^{(tg)}$ and a reference strain rate $\dot{\mathbf{E}}^0$, whose behavior is identical to the average of the polycrystal with a viscoplastic compliance $\mathbf{M}^{c(tg)}$ and a reference strain rate $\dot{\boldsymbol{\varepsilon}}^0$. This inhomogeneity has a local stress field when a uniform stress is applied to the HEM. Using the Eshelby formalism, the inhomogeneity is replaced by an 'equivalent

inclusion' having the same moduli as the polycrystal, subjected to a fictitious transformation strain rate $\dot{\boldsymbol{\varepsilon}}^*$.

The overall viscoplastic compliance moduli of the grain, $M^{(\text{sec})}$, can be calculated in a self-consistent, iterative way, as the HEM is assumed to describe the average behavior of the aggregate. This forces the weighted average of stress and strain rate over the grains to coincide with corresponding macroscopic values.

Texture evolution is simulated by enforcing the polycrystal deformation through successive incremental steps. These are obtained by imposing a macroscopic strain rate $\dot{\mathbf{E}}$ during the time interval Δt, with a guess value at each step used for the strain rate $\dot{\boldsymbol{\varepsilon}}$ in each grain. The first deformation step uses a Full Constraints guess. The stress is than calculated using Eq. (8), with each following step using the values from previous steps as the starting guesses. The macroscopic secant modulus $\mathbf{M}^{(\text{sec})}$ is estimated using the Voigt average, $\mathbf{M}^{(\text{sec})-1} = \left\langle \mathbf{M}^{c(\text{sec})-1} \right\rangle$ for the first step, with the following steps using preceding values to derive the next estimate. This modulus is then used to calculate the Eshelby tensor, $\mathbf{S}$, the interaction tensor, $\tilde{\mathbf{M}}$, and the accommodation tensor, $\mathbf{B}^c$. The average $\left\langle \mathbf{M}^{c(\text{sec})}\mathbf{B}^c \right\rangle$ is used as an improved guess for $\mathbf{M}^{(\text{sec})}$, with repeated iterations until the average coincides with the input tensor, under a certain tolerance. This value is then used to calculate the macroscopic stress

$$\boldsymbol{\Sigma}' = \mathbf{M}^{(\text{sec})-1}\dot{\mathbf{E}} \tag{9}$$

Each grain is then allowed to reorient due to slip and twinning, following a convergence criterion. The lattice rotation rate for each grain is given by

$$\dot{\omega}_{ij} = \dot{\Omega}_{ij} + \Pi_{ijkl} S^{-1}_{klmn} \tilde{\dot{\varepsilon}}_{mn} - \sum_s \frac{1}{2}(b^s_i n^s_j - b^s_j n^s_i)\dot{\gamma}^s \tag{10}$$

where $\dot{\Omega}$ is the antisymmetric component of the macroscopic distortion rate, Π is the reorientation of the associated ellipsoid, and S is the antisymmetric component of the plastic distortion rate (plastic spin); Π is proportional to the difference between the strain rate of the grain and that of the polycrystal. Tiem et al. [27] showed that for the elastic inclusion case, Π increases with ellipsoid distortion. The modeling of the grain orientation will then use the Volume Transfer Scheme as described by Lebensohn and Tome [14, 28] for twinned volume fractions. The polycrystal is represented as a discrete set of orientations. These orientations are fixed, but their representative volume fractions evolve during deformation. The Euler space is partitioned regularly in equiaxed cells or bins of 10 degrees on each side (Bunge angle convention). The orientations coincide with the centers of the cells. A certain volume fraction of the material is assigned to each cell, corresponding to the initial texture. The reorientation of lattice orientation that drives texture evolution during inelastic deformation is visualized as displacements in Euler space of the represented points. The cell as a whole displaces rigidly by an amount, and when the cell partially overlaps neighbors, the volume fraction of material in the overlap is subtracted and transferred to the neighbors. This is repeated every iteration, providing gradual texture evolution. With twinning active, a fraction of the cell adopts a new orientation and is transferred to the corresponding cell in Euler space.

The model for updating orientation based on twinning, in contrast to a pure slip model which assumes homogeneous grain deformation, assigns incremental deformation in a volume fraction of the grain [28], i.e.,

$$\Delta g^{n,t_i} = \frac{\Delta \gamma^{n,t_i}}{S} \tag{11}$$

where $\Delta g^{n,ti}$ is the volume fraction of grain n, $\Delta \gamma^{n,ti}$ is the shear strain contributed by the twinning system t_i in grain n, and S is the characteristic shear of the twin. This grain fraction is representative of the polycrystal volume fraction according to the incremental relation

$$\Delta f^{n,t_i} = f^n \frac{\Delta \gamma^{n,t_i}}{S} = f^n \Delta g^{n,t_i} \tag{12}$$

To avoid the need to increase the number of crystallite orientations, and therefore keeping the number of orientations representing the twinned fractions from geometrically increasing, Van Houtte [29] created a model wherein the grains do not increase but are assigned a criterion to either reorient by slip or belonging to one of the twinning related orientations. This criterion is based on the relative volume fraction of the twin parts versus the non-twinned parts. For the predominant twin reorientation scheme used in VPSC, a threshold formula is used for the criterion [28]

$$F_T = 0.25 + 0.25 \frac{F_E}{F_R} \tag{13}$$

where F_E is the "effective" polycrystal twinned fraction, i.e.,

$$F_E = \sum_n f^n \quad , \tag{14}$$

and F_R is the "real" twinned fraction, i.e.,

$$F_R = \sum_m f^n \sum_{t_i} g^{n,t_i} \tag{15}$$

Here, $g^{n,ti}$ is fraction of the grain associated with a twin system, t_i, which is accumulated in each deformation step that is accommodated by slip and twinning, and f^n is the volume fraction representing a grain that is completely reoriented by twinning.

At each increment of deformation, the fraction accumulating in the individual twinning system of each grain, $g^{n,ti}$, is compared against the threshold, F_T. If $g^{n,ti}$ is larger than the threshold, the grain is allowed to reorient to the twinning system. The consequence of this operation is that only the systems which exhibit the most activity will reorient by twinning. This is assumed to be correct when one twin system is dominant over the others, but may be less so when several twin systems contribute at a comparable level to deformation [28].

18

CHAPTER 3

3.1 Experimentation

Samples were machined from an α-DU cylindrical rod for mechanical and microstructure study. The DU samples were mechanically shocked at room temperature, in a manner similar to impact compression in normal direction. Samples were then ion etched for 5 hrs in Xe gas at 80°C, conducted in Model 682 Gatan Precision Etching and Coating System with voltage at 4.5 KeV and 10 rpm.   Phase analysis of α-DU samples demonstrated an orthorhombic crystal structure. Orientation imaging microscopy (OIM) was used to analyze microtexture evolution.

3.2 Simulation

Previous work on simulating texture evolution used the full constraints approach [30, 31]. This approach was compared by Lebensohn and Tome against the VPSC model, where they concluded that the VPSC model was more dependent on soft systems, with lower twinning activity, since fewer systems were active in each grain [25]. This allowed for grain interaction with the matrix, which is crucial for anisotropic materials, such as alpha uranium. Previous investigations into uranium texture were also conducted by Mitchell and Roland [32], who experimentally compared rolling samples to tension and compression predictions by Calnan and Clews [33]. Mitchell and Roland's results at low temperatures matched the previous predictions, in which there is only a single unit cell orientation producing glide by twinning alone. At higher temperatures, however, where a duplex orientation occurred in the experimental samples, there was no match with Calnan

and Clew's prediction wherein simultaneous slip and twinning was thought to occur. Reevaluation of the deformation modes at higher temperatures gave an improved texture prediction when the addition of the (010) slip system was established to become more active [32]. This could conclude that as deformation temperatures increased, different or additional deformation systems can come into increasing effect.

The active slip and twin systems used in the present simulations were taken from previous literature sources, such as Rollett [34], including the values for the critical resolved shear stress and the twinning shear. These values are simply relative to one another, as exact values of CRSS's are very limited. As noted by Rollett, [34] the results of the texture evolutions were not very sensitive to exact values, but sensitive to relative values instead. The parameters used in this study are listed in Table 1.

Table 1: Slip and twin systems used in simulations.

System	CRSS	Twinning Shear
{010}<100> Slip	0.5	-
{110}<110> Slip	1	-
{001}<100> Slip	1	-
{110}<001> Slip	99	-
{021}<112> Slip	99	-
(130)[310] Twin	0.2	0.299
(172)[312] Twin	1	0.227
(112)[372] Twin	1	0.227
(197)[512] Twin	2.5	0.216

An additional twin system except those listed in Table 1 is considered, the (176)[512] system. Experimental results show that this system is relatively more active at high strain rate deformation. CRSS of 1 and twinning shear of 0.1 were assumed for this twin system. This system is an important deformation mode for uranium, but very elusive as only appears at high strain rates, such as shock loading. Orientation distribution function plots of twice-shocked α-DU samples are shown in Figure 1. In Figure 1, each subsequent image is in steps of 18° of ϕ_2. For each image, ϕ_1 is in the x-axis of each image and Φ is in the y-axis. Components of the (176)[512] twins could be caused by the higher temperatures induced by nearly adiabatic from high strain rate deformation, as Mitchell and Roland noted that high temperatures can change the active deformation modes in uranium [32].
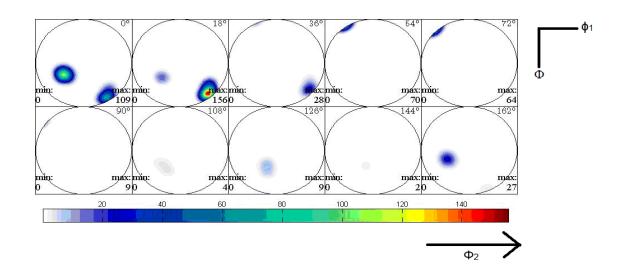

Figure 1: Experimentally measured orientation distribution function in shocked α-DU.

The high strain rate response, therefore, will include an active (176)[512] twinning mode, while slower strain rate deformation response will not. To compare the effects of the (176)[512] twinning system has on texture evolution, deformation processes are simulated in terms of quasi-static imposed deformation with and without the (176)[512] twinning. The inclusion of this system is then indicative as having been in a high strain rate deformation process, while exclusion is regarded as characteristic of low strain rate deformation for purposes of the present study.

The lattice parameters of DU samples in this study are a=2.854 nm, b=5.87 nm, and c=4.955 nm, with orthorhombic crystal structure, as measured at Y12. These measured parameters are very close to previously measured values [12]. The elastic moduli were taken from previous experimental measurements by Soderlind [35], listed in Table 2.

Table 2: Elastic moduli (GPa) for α-DU [35].

C11	C22	C33	C44	C55	C66	C12	C13	C23
2.15	1.99	2.67	1.24	0.734	0.465	0.465	0.218	1.08

Various deformation processes are simulated, including swaging, compression, tension, rolling and torsion. These processes were imposed on 500 random texture orientations using the VPSC model. This initial texture is therefore chosen as to be random, with a texture intensity less than 1.01. In this study, we first simulate texture evolution of α-uranium under swaging, compression, rolling, and torsion processes. These simulations

are validated by using data from the previous experimental study of Rollett and Morris [34, 36]. Since these experimental study were conducted at room temperature, the (176)[512] twin system is not considered in simulation. Next, several parametric simulation are performed to study the influence of activation of the (176)[512] twin system under a high strain rate process in different deformation mode. These simulations use the five previously mentioned slip systems, without (176)[512] twinning system under low strain rate and with (176)[512] twinning system under high strain rate. Finally, simulations of texture evolution under uniaxial compression with (176)[512] twin activated are compared with experimental results of shocked DU sample from Y12.

CHAPTER 4

4.1 Results

Figures 2 – 4 present results of the VPSC model for various quasistatic deformation processes, and compares simulation results with experimental results from the literature with regard to texture evolution [34, 36]. These simulations were conducted to 45% strain for swaging, 90% strain for compression, 80% strain for rolling, and 60% strain for torsion, using 2% steps for all processes. In these simulations, the {010}<100>, {110}<110>, {001}<100>, {110}<001>, and {021}<112> slip systems were active. In addition, the (130)[310], (172)[312], (112)[372], and the (197)[512] twin systems were active. For the most part, simulations agree satisfactorily with the experiments. In general, the intensity in the (010) direction had the highest level of agreement, such as with the rolling (Figure 3) and torsion (Figure 4) pole figures, while that of the other two directions, (001) and (100), exhibited less agreement.
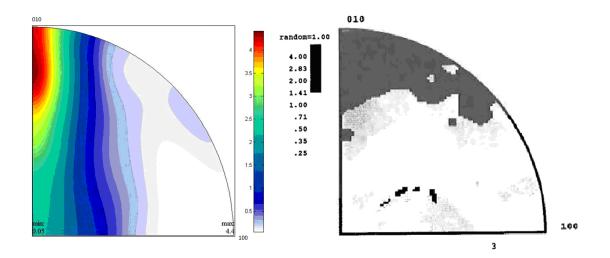
Figure 2a: Comparison of inverse pole figure of swaging process, 45% strain: (left) simulations and (right) experimental results from Rollett [34].
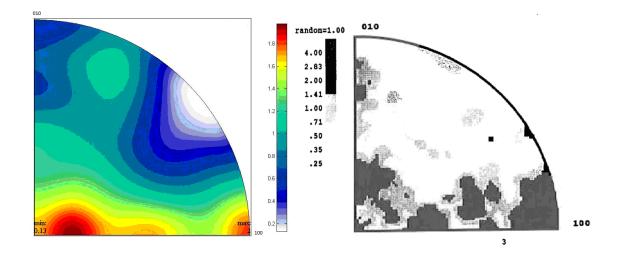

Figure 2b: Comparison of inverse pole figure of compression process, 90% strain: (left) simulations and (right) experimental results from Rollett [34].
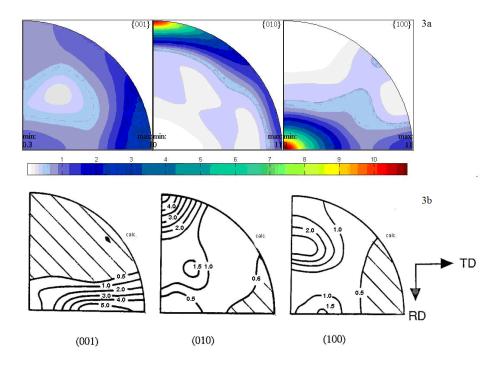
Figure 3: Comparison of pole figures of rolling process, 80% strain: 3a (top) simulations and 3b (bottom) experimental results from Morris [36].
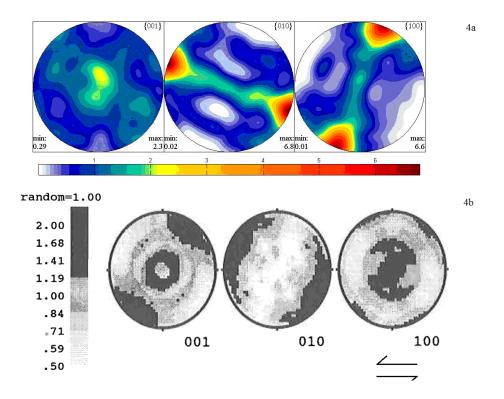

Figure 4: Comparison of pole figures of torsion process, 60% strain: 4a (top) simulations and 4b (bottom) experimental results from Rollett [34].

This suggests that there are certain limitations of the VPSC model. Specifically, as noted by Lebensohn, the volume transfer scheme does not take stress relaxation into effect. A material with an active twin undergoes stress relaxation which modifies the stress in the affected grain and its interacting matrix. As this is an elastic effect, it is beyond the scope of the current fully plastic VPSC model. In addition, twinning may also influence plastic response in the grain, a coupling the VPSC model neglects [15]. These omissions in the model may account for some of the discrepancies between simulated and experimentally measured textures.

Another aspect which may be considered is the number and type of deformation modes that were used in the simulation. The five slip and four twinning systems used in the foregoing simulations are the most commonly reported active deformation modes, but α-DU has a very high number of possible deformation modes, with around 40 theoretical twinning modes [8].

As discussed previously, the (176)[512] family of twins is much more prevalent in shocked uranium samples [24]. Certain deformation modes are strain rate dependent, with the (176)[512] system being more active at high deformation rates.

In Figures 5 – 8, comparisons are made among simulations, including swaging, compression, rolling, and torsion to 100% strain using 2% steps. In these comparisons, however, two sets of simulations were conducted with and without the (176)[512] twin system active. In this manner, the influence of the twin system can be considered for each deformation process. In general, the intensity of the texture is lowered for the simulations with (176)[512] twinning included. The exceptions to this are mainly seen in the pole figures for {010} directions. Specifically, the texture for {010} directions for compression (Figure 6), rolling (Figure 7), and torsion (Figure 8) are higher for cases with (176)[512] twinning included, especially for the cases of rolling and torsion. When the overall texture intensities are considered, however, only torsion results in an increase in overall texture. Table 3 shows the overall texture intensities for all eight cases. Torsion is the only deformation process that shows an overall increase in intensity of texture from the activation of the (176)[512] twin, which implies that if an increase in twinning from this system is preferred, a high rate torsion process should produce the greatest contribution to texture from (176)[512] twinning.

5a: No (176)[512] twinning
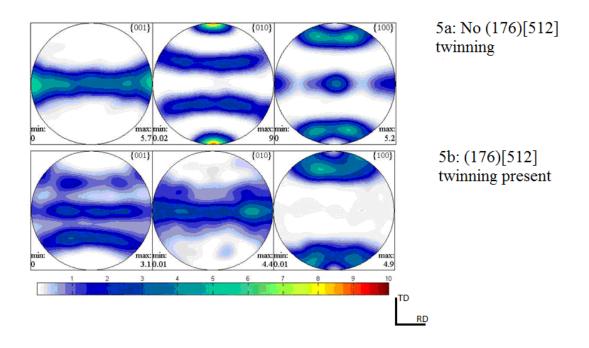
5b: (176)[512] twinning present

Figure 5: 100% swaging simulation comparisons: 5a (top) simulation with no (176)[512] twinning and 5b (bottom) simulation including (176)[512] twinning.

Figure 5 shows that when the (176)[512] system is included, there is a large drop in the overall texture intensity. The greatest drop is in the {010} pole figure; the strong texture at the poles are completely absent in when (176)[512] twinning is included.
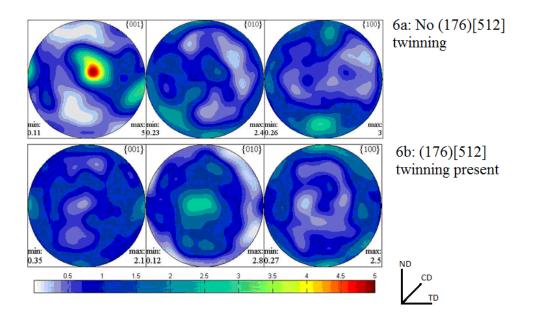
Figure 6: 100% compression simulation comparisons: 6a (top) simulation with no (176)[512] twinning and 6b (bottom) simulation including (176)[512] twinning.

For the case of compression (Figure 6), the only significant development of texture lies in the {001} pole figure in the absence of (176)[512] twinning. With active (176)[512] twinning, the texture near the center of the pole figure is completely absent.

Figure 7: 100% rolling simulation comparisons: 7a (top) simulation with no (176)[512] twinning and 7b (bottom) simulation including (176)[512] twinning.

Rolling textures differ when the (176)[512] system is activated. For the {001} pole figure, the strong texture at the edges is absent in when (176)[512] twinning is included.. Conversely, strong textures appeared in the {010} pole figure when the (176)[512] twin system is active.
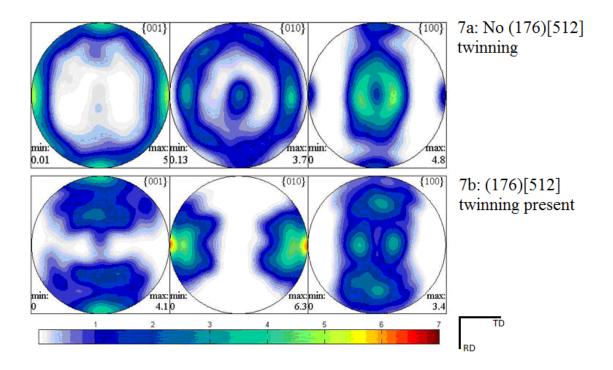
Figure 8: 100% torsion simulation comparisons: 8a (top) simulation with no (176)[512] twinning and 8b (bottom) simulation including (176)[512] twinning.

Torsion is an interesting case for comparison. The pole figures in Figure 8 exhibit no strongly textured regions as in the previous three cases. Instead, the {001} and {100} pole figures decreased in intensity, while the {010} pole figure increased. Noting Table 3, it can be seen that the torsional deformation was the only one in which there was an overall increase in the intensity of texture as the (176)[512] system became active.

Table 3: Comparison of intensities in pole figures from Figures 5-8.

Process	Texture Index ((176) not active)	Texture Index ((176) active)
Swaging	6.6	5.1
Compression	2.5	1.7
Rolling	4.3	4.1
Torsion	3.5	4.3

As a final demonstration of the versatility of the VPSC model, an experimentally shocked sample of α-DU from Y12 was simulated to produce similar textures. As the sample was mechanically shocked in a single loading direction, a quasistatic compression process was used with deformation to 100% strain. The shock deformation solicited the (176)[512] twinning mode in experiments, along with {110}<110> slip systems. These two deformation modes were considered in the simulation, using a relative CRSS of 1 and twin shear of .1 for the (176)[512] twin system, and a relative CRSS of 1 for the {110}<110> slip system.   The result of the simulation is compared with the experimentally measured texture in Figure 9. As can be seen, the simulation compares closely to the experimentally measured texture.
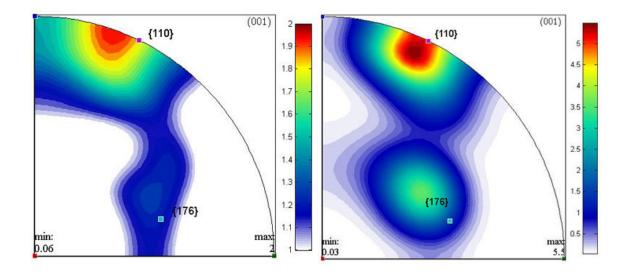
Fig 9: Comparison of inverse pole figures of simulated (left) and experimentally measured (right) textures for shock compression.

4.2 Discussion

From the simulations of swaging, compression, rolling and torsion processes, the VPSC model was shown to model the experimental results satisfactorily. Different directions appear to have greater amounts of similarity to the experimentally measured textures, with the (010) direction being the most accurate, in general. This is due to certain limitations in the VPSC model, most notably that it disregards elastic deformation and stress relaxation. Previous sources have reached similar conclusions on the limitations of the VPSC model discounting elastic deformation, especially on the effects of the elastic regime on twinning [15].

When the (176)[512] twin is activate within the simulation, there is a decrease in texture intensity in most deformation processes, except for torsion, which shows an increase in the overall texture. Specific orientations in both torsion and rolling increase in texture while others decrease. It would appear, in general, that this twin system suppressed the texture intensities for the most of the deformation processes. The only deformation process where the intensity increased was for torsional deformation. This twin system then, although a dominant deformation mode, may be hampering the other deformation slip and twin systems, leading to an overall decrease in the intensity of texture. This could come from the effects of pinning that this twin system may produce. As this twin system is more prevalent in samples which are subjected to high strain rates, the (176)[512] twin may surface as a dominant deformation mode, and then, by pinning twin boundaries, prevent further propagation of texture.

The VPSC model was able to simulate the sample from ORNL Y12, by increasing the strain rate of the original simulations and by limiting which deformation modes were active. With only the {110}<110> slip system and the (176)[512] twin system active, the resulting simulated texture very closely matched the experimentally measured texture. However, since the VPSC model cannot simulate very high rates of deformation, the texture intensities of the simulation were much lower than the experiment. The close match in the simulation when only these two deformation modes were active seem to imply that for the mechanically shocked sample, only these systems were able to become active or that they were much more dominant than the other deformation modes.

4.3 Conclusion

The viscoplastic self-consistent model is a highly efficient, very flexible, and relatively robust model for texture simulation. Most of the simulations of the deformed uranium textures using 500 grain orientations were completed in less than fifteen minutes. The model is capable of representing materials of low symmetry and including both slip and twin systems, such as alpha uranium, which is of orthorhombic symmetry and contains many twin modes.

The (176)[512] twin is a not commonly observed in quasistatic deformation of DU, and typically is observed in samples subjected to mechanical shock loading. It is presently unclear whether the shock deformation itself or its associated nearly adiabatic temperature rise induces this twinning mode. Previous experiments have shown (176)[512] twins in uranium which underwent a γ to α phase change [24]. Hence, the effect of the (176)[512] twin system on the texture evolution of uranium may not be as simple as just comparing the overall texture. Specific pole figures should be analyzed to assess the effect the (176)[512] twin system.

The (176)[512] twinning is an interesting case of how an uncommon twin system for alpha uranium changes the texture evolution of the material. Experimental samples of uranium from ORNL Y12, which contain the (176)[512] twins, show a very strong

intensity of texture. As these samples were mechanically shocked to produce these twins, there may be a correlation in texture intensity for these twins at higher strain rates. This could be caused either directly by dynamic deformation, or by a phase change enhanced by an increase in sample temperature caused by the high rate of deformation.

References

1. Zoellner, T., *Uranium: War, Energy, and the Rock that Changed the World,* 2009, London: Penguin Books, Ltd.

2. OECD Nuclear Energy Agency, *Forty Years of Uranium Resources, Production and Demand in Perspective*, 2006, OECD Publishing.

3. Howard, S.M., *Encyclopedia of Materials: Science and Technology,* 2008. 9458 – 9459.

4. Hampell, C.A., *Rare Metals Handbook.* 2 ed., 1961.

5. Gale, W. F. and Totemeier, T. C., *Smithells Metals Reference Book.* 8 ed., 2004.

6. Cardarelli, F., *Materials Handbook: a Concise Desktop Reference*2008: Springer-Verlag London Limited. 437.

7. Loewenstein, P., *Metals Handbook.* Vol. 3. 1992: American Society for Metals. 773-779.

8. Crocker, A.G., *The Crystallography of Deformation Twinning in Alpha Uranium.* Journal of Nuclear Materials, 1965. **16**: p. 306-326.

9. Kocks, U. F., Tome, C. N., and Wenk, H. R., *Texture and Anisotropy: Preferred Orientations and Their Effect on Materials Properties,* 1998, Cambridge: Cambridge University Press.

10. Smallman, R. E., and Bishop, R. J., *Modern Physical Metallurgy and Materials Engineering,* 2002, Oxford: Elsevier Science Ltd.

11. Pitteri, M. and Zanzotto, G., *Continuum Models for Phase Transitions and Twinning in Crystals,* 2003, Boca Raton: CRC Press LLC.

12. Cahn, R.W., *Plastic Deformation of Alpha Uranium: Twinning and Slip.* Acta Metallurgica, 1953. **1**.

13. Hertzberg, R.W., *Deformation and Fracture Mechanics of Engineering Materials.* Forth ed., 1996: John Wiley and Sons, Inc.

14. Lebensohn, R.A., and Tome, C. N. , *Modelling Twinning in Texture Development Codes.* Textures and Microstructures, 1991. **14-18**: p. 959-964.

15. Lebensohn, R.A., and Tome, C. N. , *A Self-Consistent Viscoplastic Model: Prediction of Rolling Textures of Anisotropic Polycrystals.* Materials Science and Engineering, 1995. **A175**: p. 71-84.

16. Molinari, A., Canova, G. R., and Ahzi, S., *A Self Consistent Approach of the Large Deformation Polycrystal Viscoplasticity.* Acta Metall., 1987. **35**(12): p. 2983-2994.

17. Canova, G.R., *Theory of Torsion Texture Development.* Acta Metall., 1984. **32**: p. 211-226.

18. Kocks, U., Canova, G., et al. , *Yield Vectors in FCC Crystals.* Acta Metall., 1983. **31**: p. 1243-1252.

19. Kocks, U., Argon, A. and Ashby, M. , *Thermodynamics and Kinetics of Slip.* Prog. Mat. Sci., 1975. **19**: p. 1.

20. Asaro, R., and Needleman, A., *Texture Development and Strain Hardening in Rate Dependent Crystals.* Acta Metall., 1985. **33**: p. 923-953.

21. Honneff, H., and Mecking, H. , *A Method for the Determination of the Active Slip Systems and Orientation Changes During Single Crystal Deformation.* ICOTOM-5, 1978. **1**: p. 265.

22. Kocks, U., and Canova, G. . *How Many Slip Systems and Which?* in *Second Riso Int. Symposium on Metallurgy and Materials Science*. 1981. Riso, Denmark.

23. Kocks, U., and Chandra, H. , *Slip Geometry in Partially Constrained Deformation.* Acta Metall., 1982. **30**: p. 695-709.

24. Zuev, Y.N., Kabanova, I. G., Sagaradze, V. V., Pecherkina, N. L., Podgornova, I. V., and Mukhin, M. L., *Types of Twins and the Dislocation Structure of Alpha Uranium in the Initial and Explosion-Deformed States.* The Physics of Metals and Metallography 2008. **106**(1): p. 97-109.

25. Lebensohn, R.A., and Tome, C. N. , *A Self Consistent Anisotropic Approach for the Simulation of Plastic Deformation and Texture Development of Polycrystals: Application to Zirconium Alloys.* Acta. Metall. Mater., 1993. **41**: p. 2611.

26. Lequeu, P., Gilormini, P., Montheillet, F., Bacroix, B., and Jonas, J. J., *Yield Surfaces for Textured Polycrystals—I. Crystallographic Approach.* Acta Metall., 1987. **35**.

27. Tiem, S., Berveiller, M., and Canova, G. R., *Grain Shape Effects on the Slip System Activity and on the Lattice Rotations.* Acta Metall., 1986. **34**(11).

28. Tome, C.N., Lebensohn, R. A., and Kocks, U. F., *A Model for Texture Development Dominated by Deformation Twinning: Application to Zirconium Alloys.* Acta Metallurgica, 1991. **39**: p. 2667.

29. Houtte, P.V., *Simulation of the Rolling and Shear Texture of Brass by the Taylor Theory Adapted for Mechanical Twinning.* Acta Metall., 1978. **26**: p. 591.

30. Taylor, J.I., *Plastic Strain in Metals.* J. Inst. Metals, 1938. **62**: p. 307.

31. Bishop, J.F.W., and Hill, R. , *A Theory of the Plastic Distortion of a Polycrystalline Aggregate Under Combined Stresses.* Phil. Mag., 1951. **42**: p. 414.

32. Mitchell, C.M., and Roland, J. F. , *Preferred Orientation in Alpha-Uranium.* Acta Metallurgica, 1954. **2**: p. 559-572.

33. Calnan, E.A., and Clews, C. J. B., Phil. Mag., 1952. **43**: p. 93.

34. Rollett, A.D., Lowe, T. C., Follansbee, P. S., and Daehn, G. eds., *Comparison of Experimental and Theoretical Texture Development in Alpha-Uranium.* Published by TMS (Warrendale) as proceedings of symposium on "Modeling the Deformation of Crystalline Solids.", 1991: p. 361.

35. Soderlind, P., *First Principles Elastic and Structural Properties of Uranium Metal.* Physical Review 2002. **66**.

36. Morris, P.R., *Crystallite Orientation Analysis for Materials with Tetragonal, Hexagonal, and Orthorhombic Crystal Symmetries.* Proc. ICOTOM-1, 1971: p. 87.